

# THE RADIO CONTINUUM OF THE LARGE MAGELLANIC CLOUD

## I. THE SOURCES AT 6 CM WAVELENGTH

By R. X. MCGEE,\* J. W. BROOKS,\* and R. A. BATCHELOR\*

[Manuscript received 27 March 1972]

### *Abstract*

The Large Magellanic Cloud has been surveyed in the radio continuum at a wavelength of 6 cm with the 4' arc beam of the Parkes radio telescope. A catalogue of 95 sources and diagrams of their brightness contours are presented here.

## I. INTRODUCTION

The radio astronomical investigation of the continuum radiation from our nearest neighbouring galaxy, the Large Magellanic Cloud (LMC), dates from 1953, when 309 cm wavelength emission was detected by Little and Sheridan using their pilot model cross-aerial (Mills and Little 1953). Important contributions were made by Mathewson and Healey (1964) with measurements at wavelengths of 73 and 21 cm. Le Marne (1968), Clarke (1971), and Mills and Aller (1971) have observed a few of the more important sources at 73 cm.

The present series of four papers treats the radio continuum emission from the LMC as follows. This paper gives contour diagrams of the LMC at 6 cm wavelength together with a catalogue of 95 continuum sources. Part II (Broten 1972, present issue pp. 599–612) gives contour diagrams of both the LMC and SMC at 11 cm; these observations have been briefly reported by Broten (1965). Part III (McGee, Brooks, and Batchelor 1972, present issue pp. 613–17) gives a catalogue of sources at 11 cm. Part IV (McGee and Newton 1972, present issue pp. 619–35) discusses the spectra of about 60 sources and suggests possible identifications.

## II. EQUIPMENT AND MEASURING TECHNIQUES

The observations were made with the 64 m telescope at the Parkes Observatory. The radiofrequency part of the receiving equipment, on loan from the National Radio Astronomy Observatory, Green Bank, U.S.A., consisted of a low-noise cryogenic parametric amplifier followed by two tunnel-diode amplifiers. The general characteristics of this receiver have been described by Reifenstein (1968). The bandwidth was approximately 150 MHz centred on 5009 MHz and the system noise temperature was estimated to be 120 K. With an output time constant of 1 s, peak to peak noise fluctuations were less than 0.1 K. The receiver was operated in a Dicke-switched mode using a cold load as reference. The output was connected to a fast rise-time post-detector filter (Cooper 1970), which caused smaller reductions in the signal peak for the same noise-fluctuation smoothing at a given scanning rate

\* Division of Radiophysics, CSIRO, P.O. Box 76, Epping, N.S.W. 2121.

and thus substantially reduced the observing time when compared with standard *RC* time constant networks. In addition, this filter when used with two combinations of effective time constant and telescope scanning rate (0.8 s at  $1^\circ \text{ min}^{-1}$  and 4.0 s at  $0.2^\circ \text{ min}^{-1}$ ) caused a reduction of only 0.3% in the output deflection due to a source. The apparent displacements in position caused by the filter were checked by comparing forward and reverse scans on strong point sources. The errors in position resulting from the output filter and from noise fluctuations were negligible compared with those due to uncertainty in telescope pointing. At the time of this survey no accurate radio source position calibrations were known within  $30^\circ$  of the LMC. The maximum uncertainty in the telescope position indicators is believed, however, to be less than  $1'$  arc.

The primary feed aerial was a two-hybrid-mode corrugated horn structure which has been described by Thomas (1970). The aperture efficiency of the 64 m telescope at 5000 MHz was 0.4, which for optimum focus settings, changed by less than 10% over the range  $0^\circ$  to  $60^\circ$  in zenith angle. Where necessary, corrections have been made for the variation of the effective area with zenith angle using data kindly provided by D. E. Yabsley (personal communication).

The radio sources Hydra A (0916—11) and PKS 1934—63 were used to measure the aerial beam and to calibrate the flux density scale. Beam and intensity calibration measurements were made at zenith angles between  $24^\circ$  and  $56^\circ$  with the feed set alternately at orthogonal position angles. The symmetry of the aerial beam was assessed by scanning the two calibrator sources at constant declination and right ascension. In each of these directions, the beam was found to have a half-power width of  $4'.0 \pm 0'.02$  arc. The areas of the “declination beam” and “right-ascension beam” out to abscissae of  $12'$  arc were equal to within 0.9%. A Gaussian curve with the same half-intensity width and cut off at the same abscissae values had an area greater than the declination beam by 2.2% and greater than the right-ascension beam by 3.1%.

The worst side lobe was reported by Yabsley (personal communication) to be a third-order coma effect of less than  $-18$  dB at zenith angles near  $30^\circ$  but increasing to  $-13$  dB at zenith angle  $60^\circ$ . This was displaced in zenith angle by  $6'.2$  arc below the main beam. Since all the sources in the LMC are of relatively low intensity the effects of side lobes were not detectable above the receiver noise.

The scales of brightness temperature and flux density were determined for each set of observations by means of the deflection produced by a noise signal from an argon discharge tube injected into the front end of the receiver. This calibration was made at intervals of approximately 30 min. It was found that the overall receiver gain had an average variation of 3% over a 14 hr observing period. The noise tube deflection was calibrated each day by the observation of Hydra A, whose flux density at 6 cm was assumed to be 13.0 f.u.\*

For the purpose of constructing contour maps the results of the observations were expressed in terms of the full-beam brightness temperature  $T_b$ . For a point source, the relation between the flux density  $S$  (f.u.) and  $T_b$  (K) is

$$S = 1.19 T_b \quad (1)$$

\* 1 flux unit (f.u.) =  $10^{-26} \text{ W m}^{-2} \text{ Hz}^{-1}$ .

when integrated over the full-beam solid angle. Thus the full-beam brightness temperature for Hydra A was taken as 11.0 K.

On two nights the observations were obviously affected by rain and heavy cloud. These observations were repeated later in the survey.

### III. 6 CM CONTINUUM CONTOURS

A finding survey at  $1^\circ \text{ min}^{-1}$  was made over the area of sky containing the LMC and extending from R.A.  $04^{\text{h}}40^{\text{m}}$  to  $06^{\text{h}}10^{\text{m}}$  and from Dec.  $-63^\circ$  to  $-75^\circ$ . Between Dec.  $-63^\circ$  and  $-70^\circ$  the scans were made at intervals of 30 s in right ascension (equivalent to  $\sim 3'$  arc) and between Dec.  $-69^\circ$  and  $-75^\circ$  at 45 s in right ascension (or  $\sim 3' \cdot 5$  arc). All regions in which any evidence of continuum emission was noted in the finding survey were then scanned at intervals of half the aerial beamwidth ( $2'$  arc) using slower speeds and appropriate receiver gain settings. The scans in right ascension were made in the larger regions of emission; important long tie scans were made at Dec.  $-69^\circ 05'$ ,  $-69^\circ 10'$ ,  $-69^\circ 30'$ , and  $-69^\circ 45'$ . The boundaries along Dec.  $-63^\circ$  and  $-75^\circ$  and along R.A.  $06^{\text{h}}10^{\text{m}}$  were regarded as regions of zero on the temperature scale. Since all scans were relatively short the effects of changing ground and atmospheric radiation with zenith angle were negligible.

At the resolution of this survey ( $4'$  arc) the LMC appears as a series of individual sources except for a large complex of sources and background radiation in the immediate vicinity of the 30 Doradus nebula. Contour diagrams of the regions of 95 sources observed in the survey area are given in Figures 1–11. The contour interval is 0.1 K in full-beam brightness temperature. The peak temperature is indicated on each source. For source MC 39 (Fig. 5) the contour interval changes to 0.2 K above 1 K; for MC 74 (Fig. 11) the intervals above 1.0 K are as marked (this area is indicated by stippling). The peak brightness temperature of 12.6 K for MC 74 far exceeds that of any other source in the region. Only six of the sources have brightness temperatures exceeding 1 K.

The sources have been numbered in order of increasing right ascension, and these numbers are shown beside the sources in the figures. It was found convenient to group the sources in the diagrams in the manner shown, and some sources thus occur out of numerical order. The sources included in each figure are listed in the captions. Weak sources whose existence is somewhat doubtful are shown with broken contour lines.

### IV. SOURCE CATALOGUE

The sources and some of their physical characteristics are listed in Table 1. Columns 1 to 3 give the catalogue number and the position of the peak of each source; the position in right ascension and declination is referred to epoch 1950.0. The maximum full-beam brightness temperature of the source is listed in column 4.

The half-power widths of the sources in right ascension and declination given in columns 5 and 6 have been derived from the measured half-widths, assuming both the source and the antenna beam to be Gaussian in shape. The average error of the measured half-widths is estimated as  $\pm 0' \cdot 05$  arc, so that if the measured width was  $< 4' \cdot 05$  arc we have given the derived size as  $< 0' \cdot 7$  arc instead of merely stating "point source". Dashes in these columns indicate that a source was too weak for its half-width to be measured.

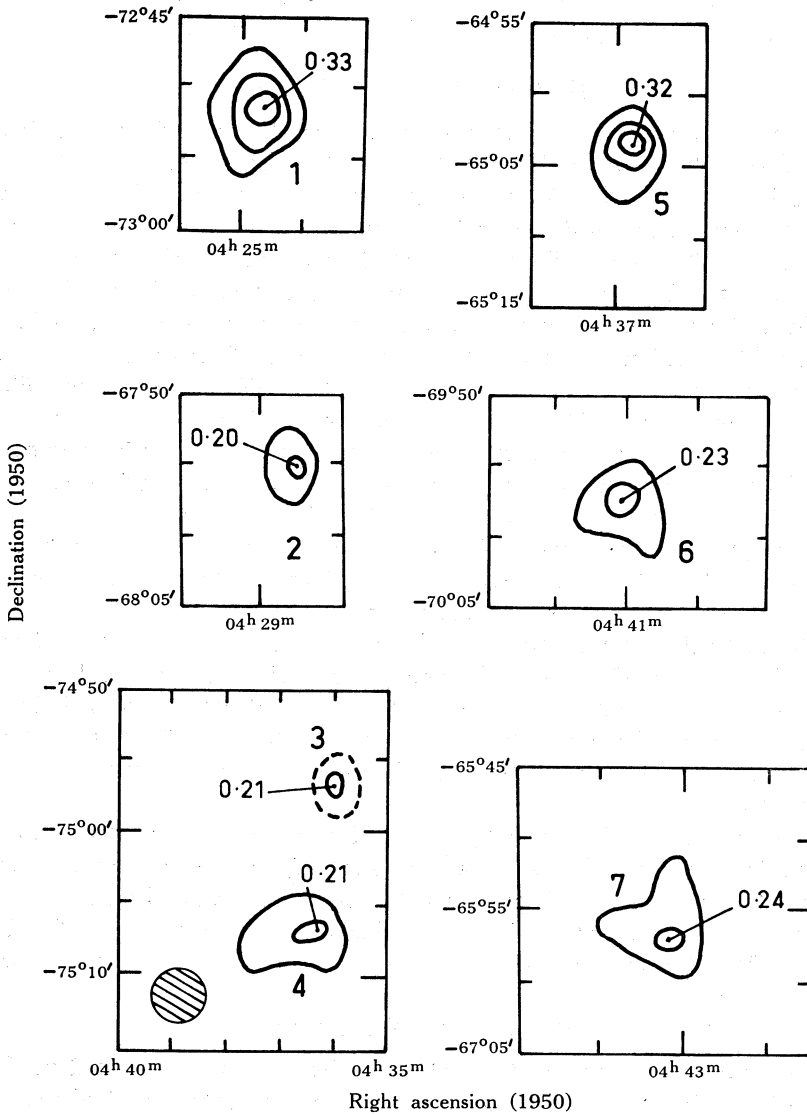


Fig. 1.—MC 1–7.

Figs. 1–11.—Contour maps of the radio sources in the LMC at 5009 MHz (6 cm). The contour interval is  $0.1$  K full-beam brightness temperature, from  $0.1$  K. The maximum value of  $T_b$  is marked on each source. The aerial beamwidth at half power was  $4'.0$  arc, and is shown by the hatched circle. The large numerals on the contour maps correspond to the catalogue numbers (MC omitted). The sources included in each figure are listed in the individual captions.

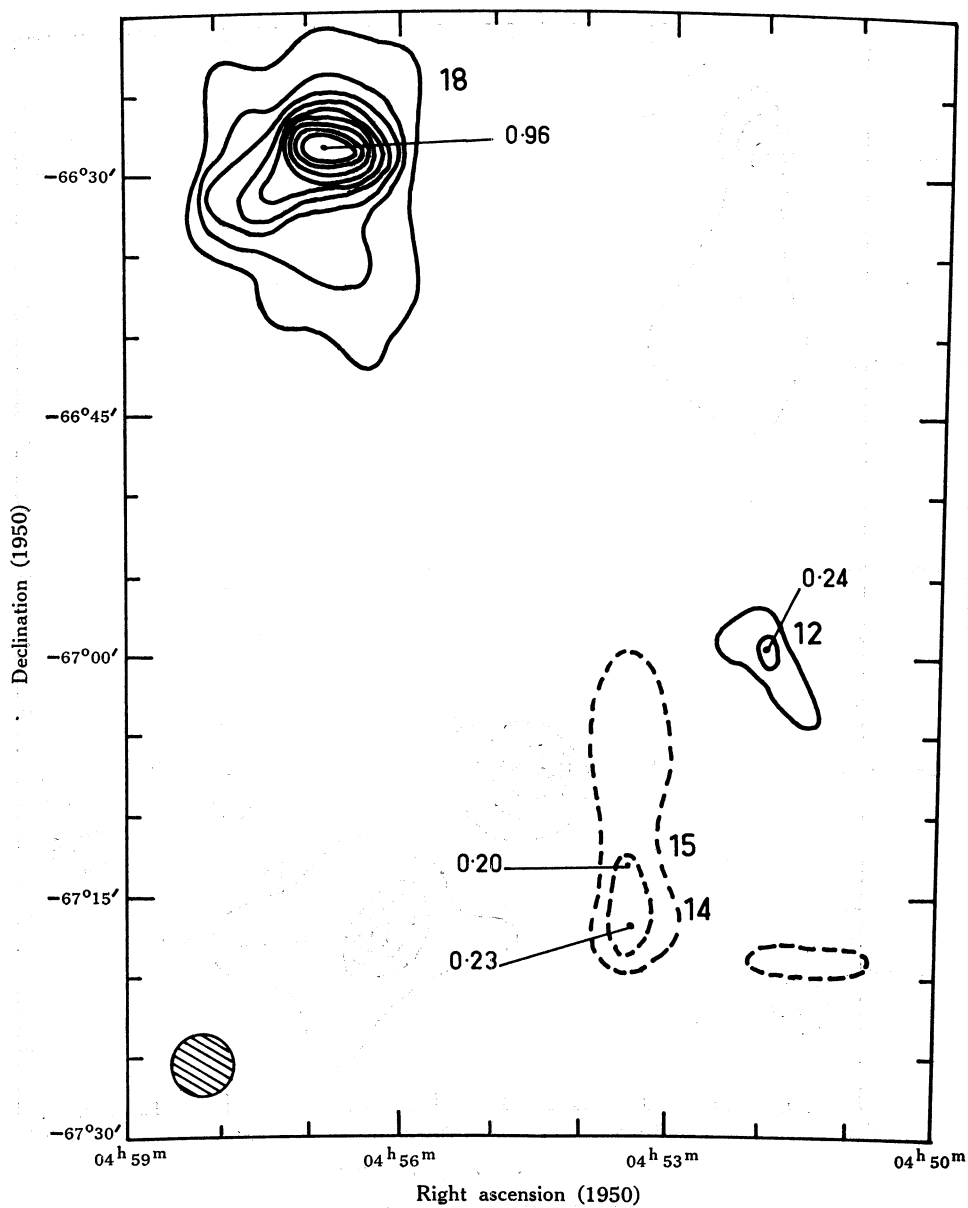


Fig. 2.—MC 12, 14, 15, 18.

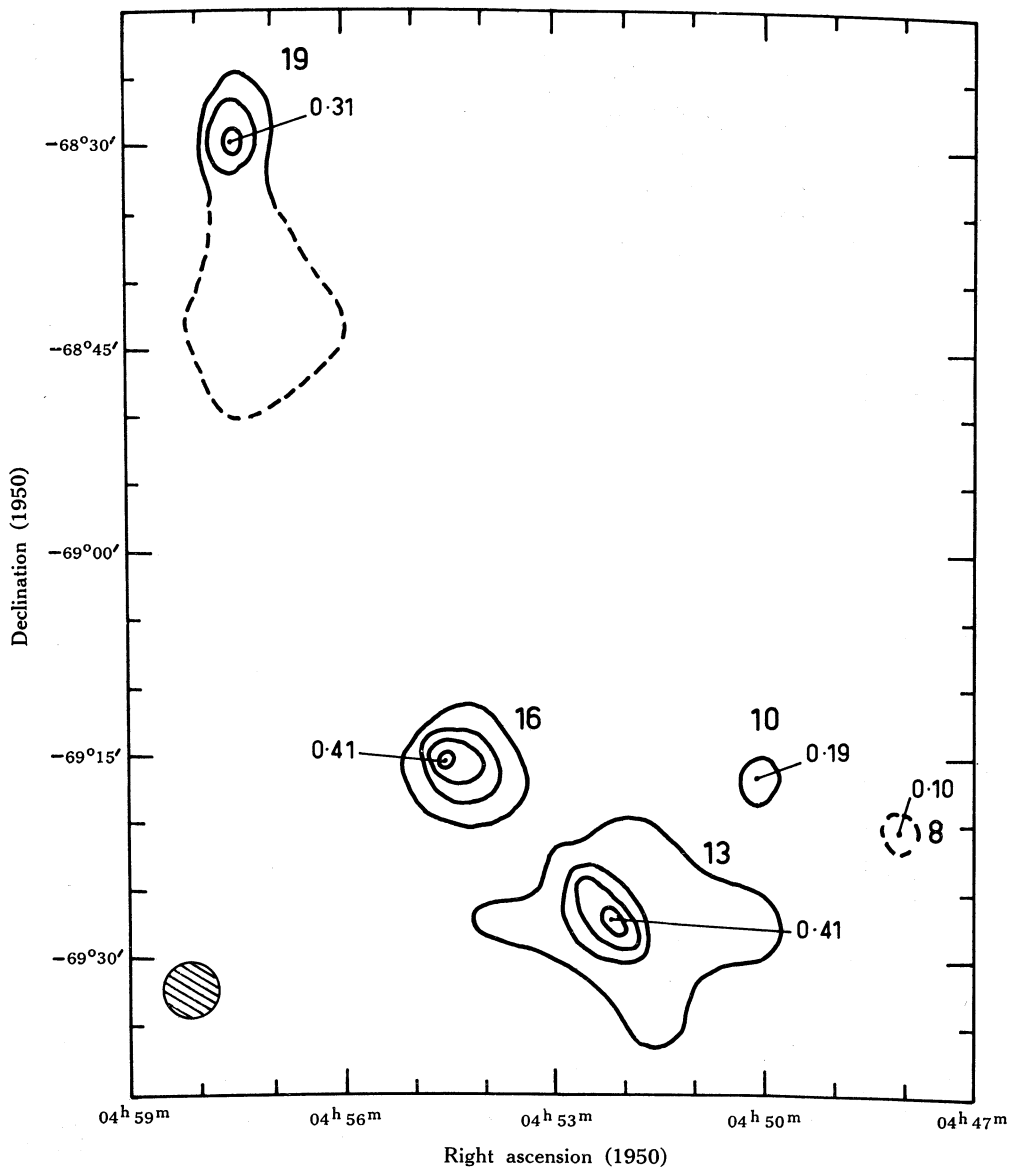


Fig. 3.—MC 8, 10, 13, 16, 19.

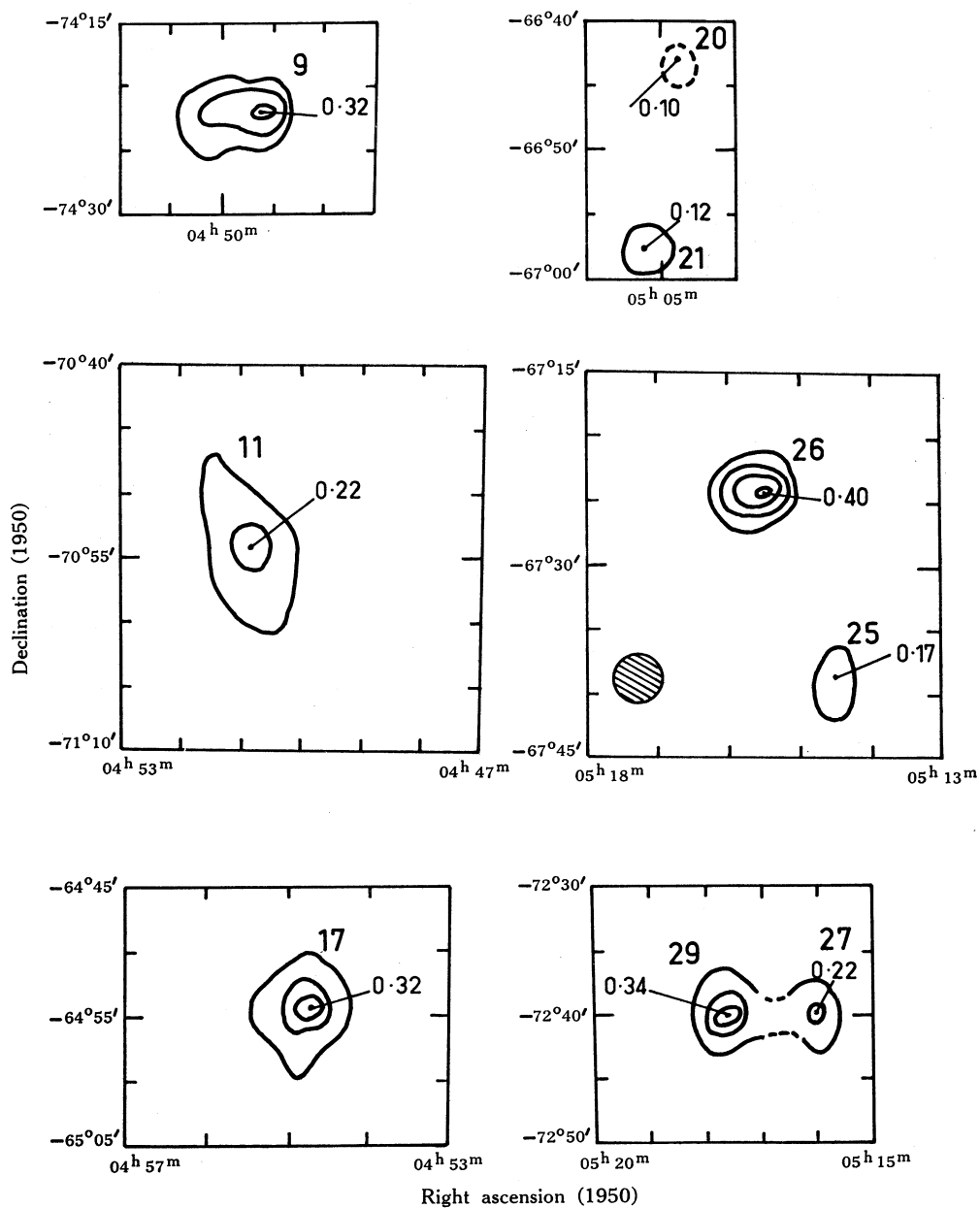


Fig. 4.—MC 9, 11, 17, 20, 21, 25, 26, 27, 29.

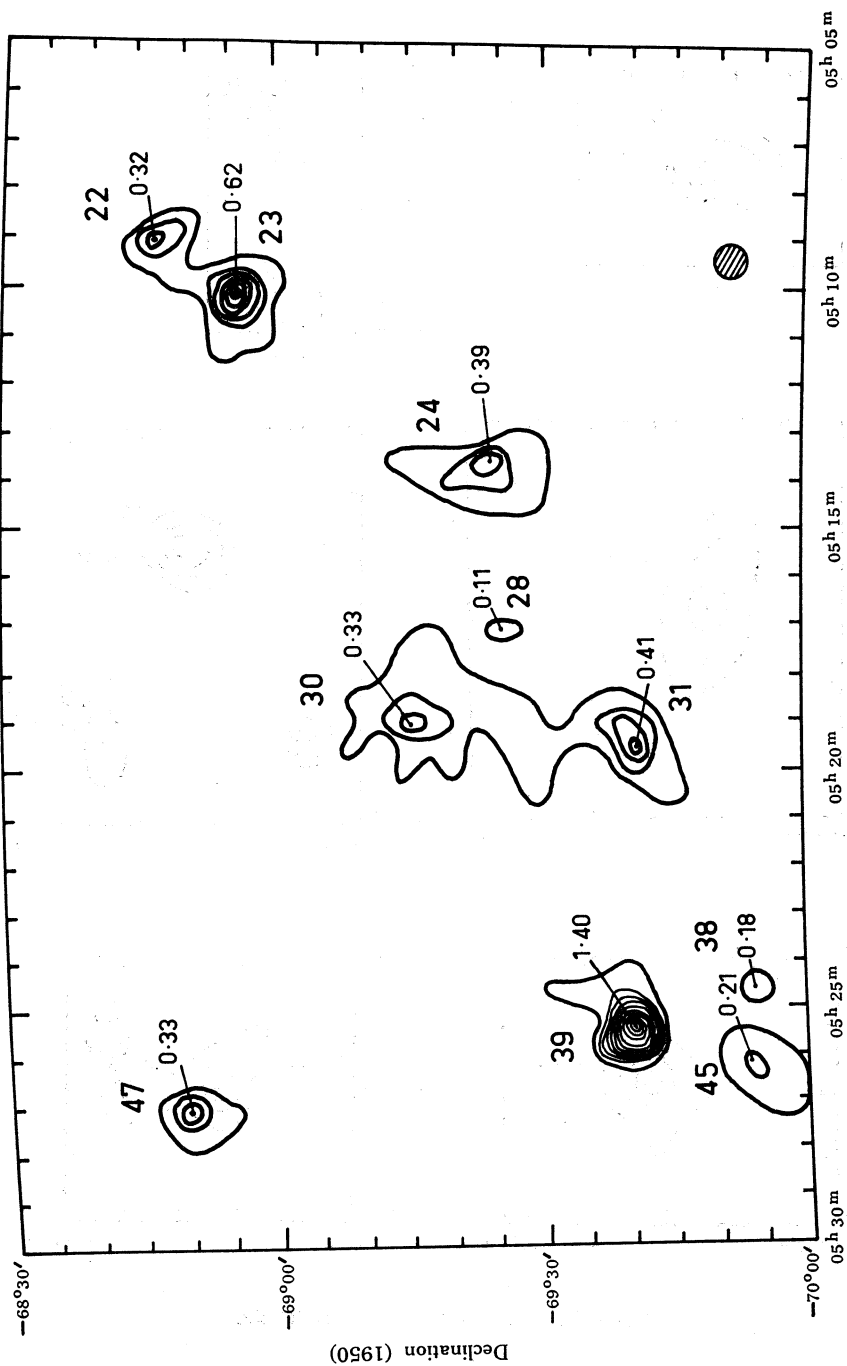


Fig. 5.—MC 22, 23, 24, 28, 30, 31, 38, 39, 45, 47.  
Right ascension (1950)



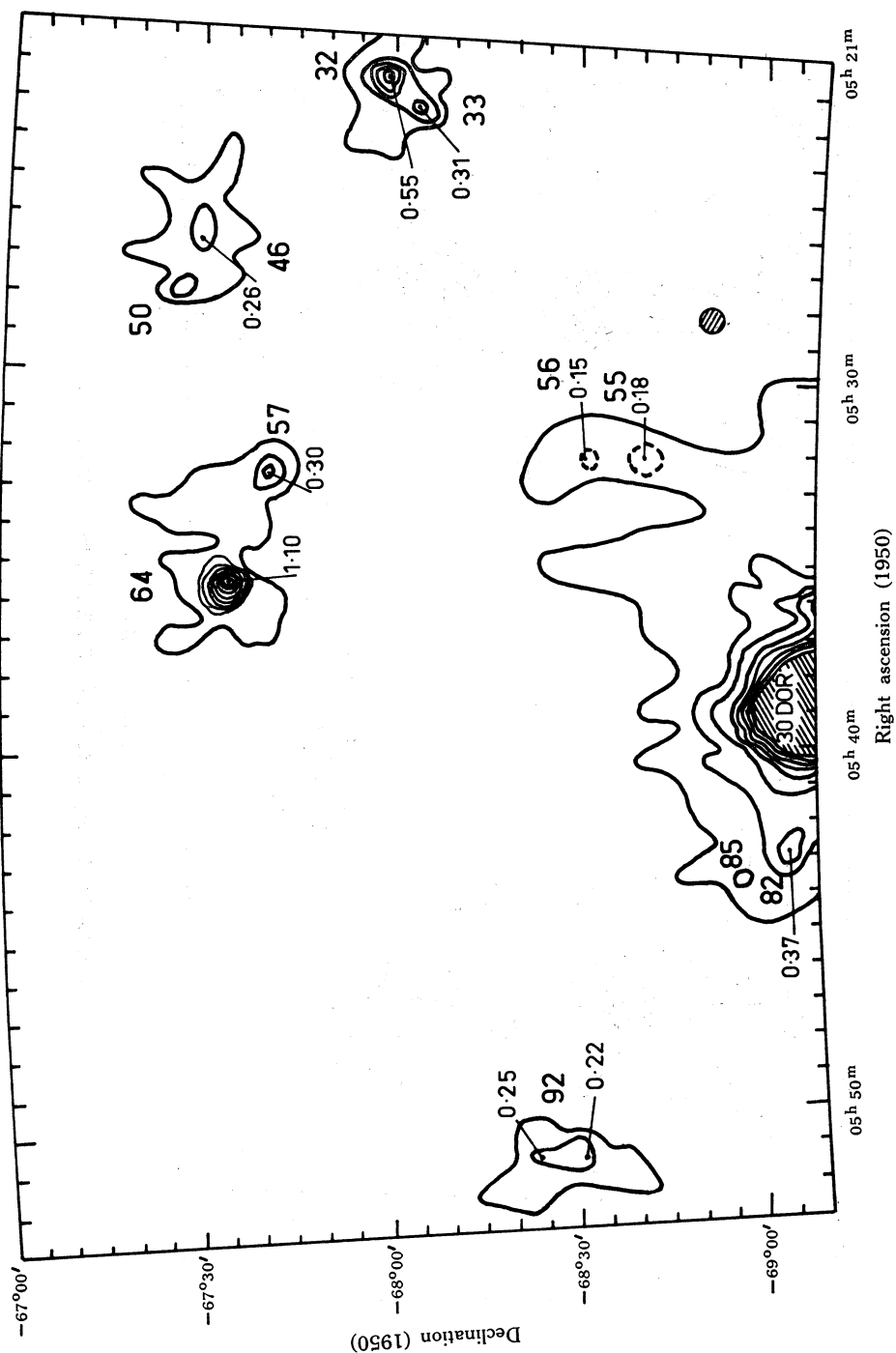
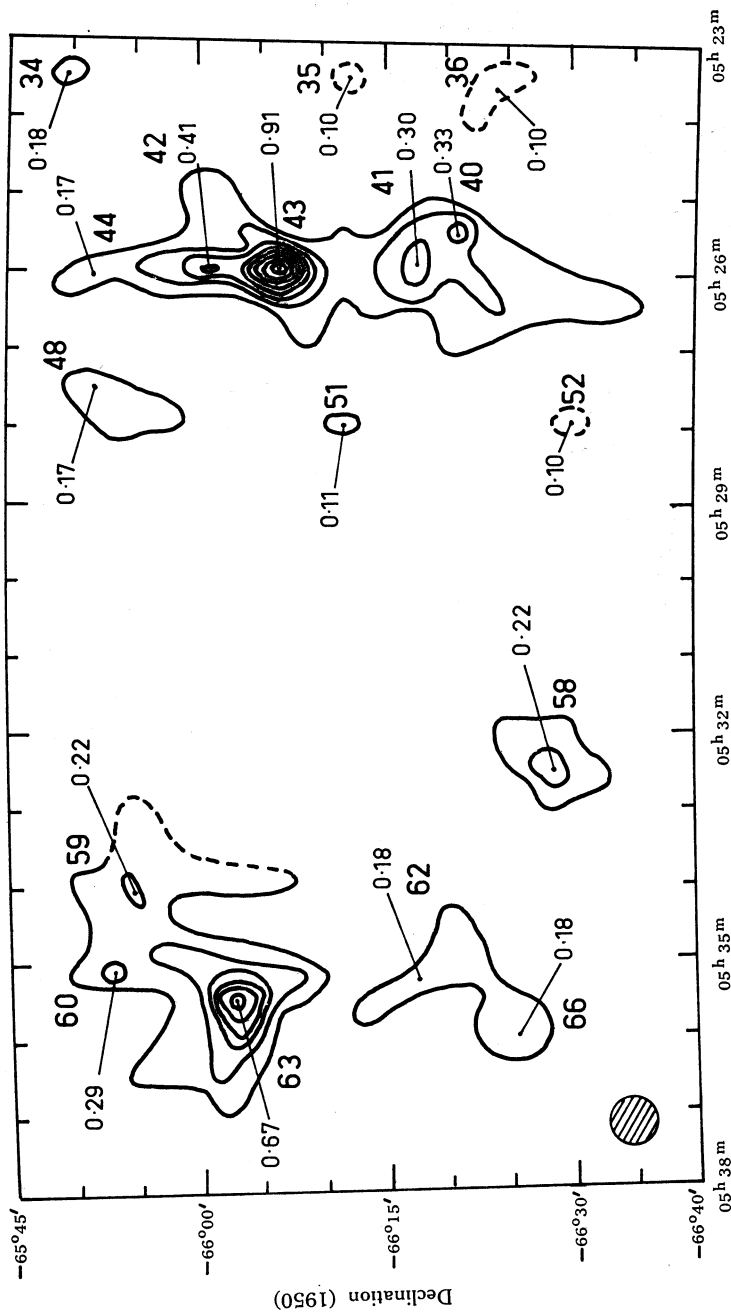
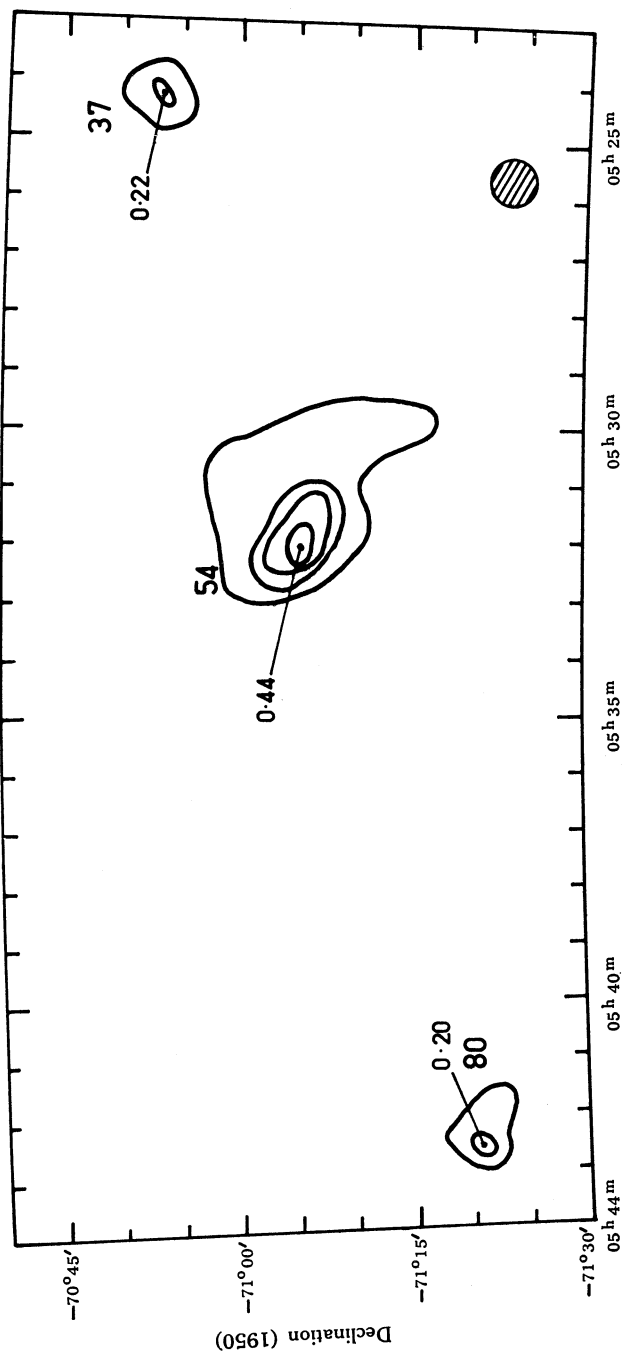


Fig. 6.—MC 32, 33, 46, 50, 55, 56, 57, 64, 82, 85, 92.



Right ascension (1950)

Fig. 7.—MC 34, 35, 36, 40-44, 48, 51, 52, 58, 59, 60, 62, 63, 66.



Right ascension (1950)

Fig. 8.—MC 37, 54, 80.

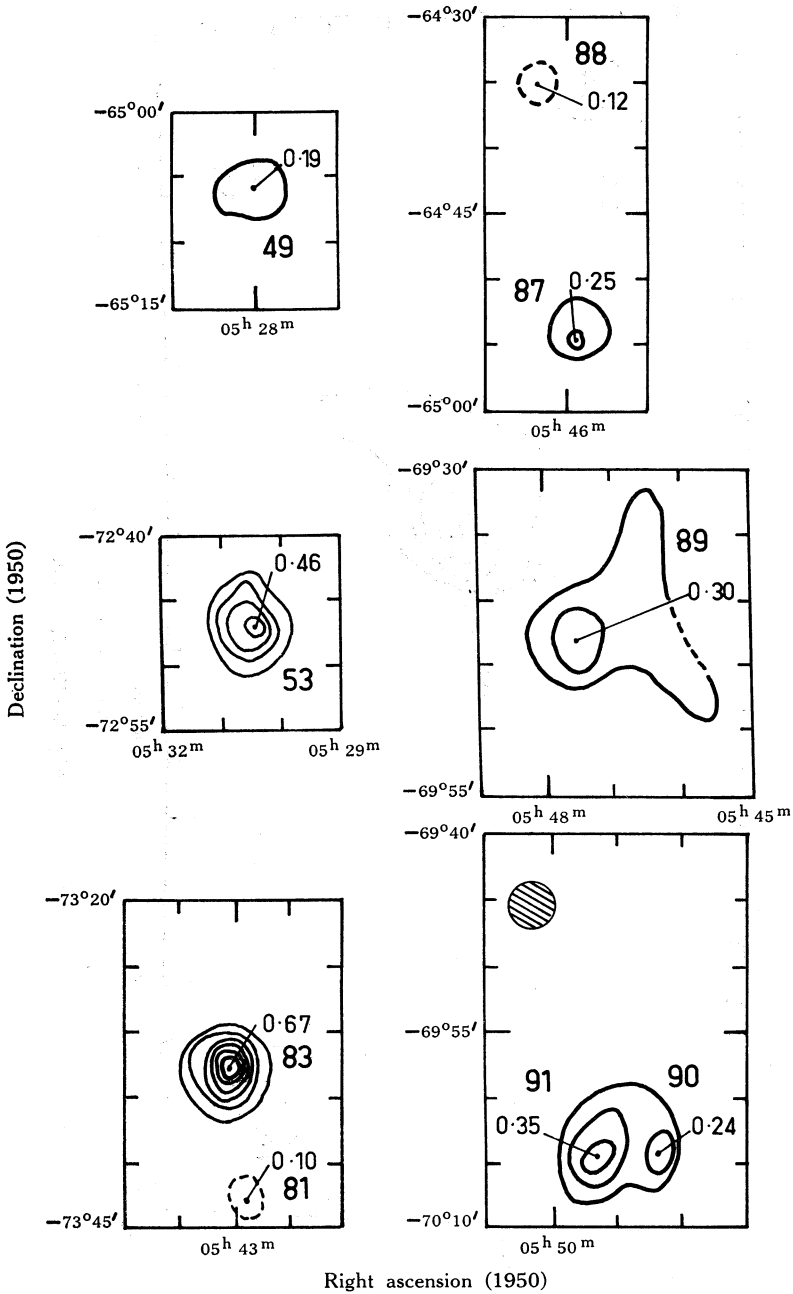


Fig. 9.—MC 49, 53, 81, 83, 87–91.

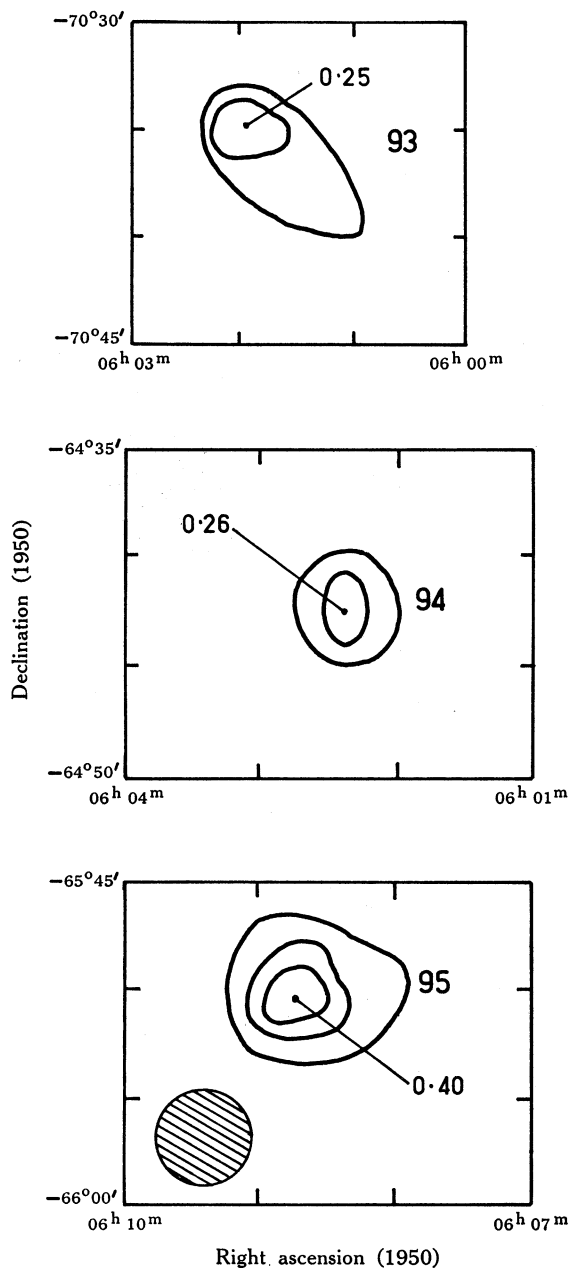


Fig. 10.—MC 93, 94, 95.

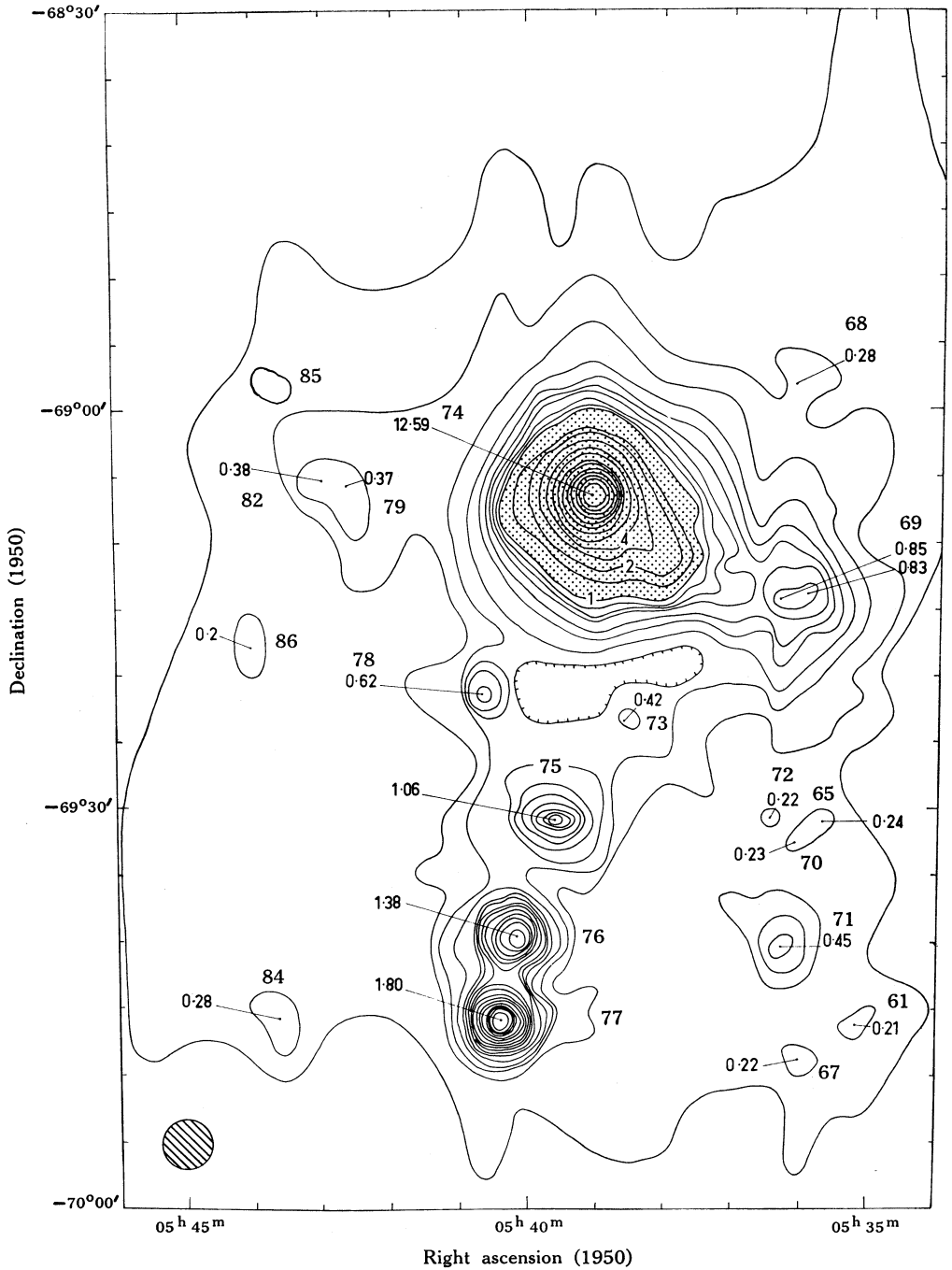


Fig. 11.—MC 61, 65, 67–79, 82, 84, 85, 86. In the stippled region the contour interval is increased to  $\sim 1$  K.

TABLE 1  
CATALOGUE OF 6 CM SOURCES IN LMC

(1)	(2)	(3)	(4)	(5)	(6)	(7)	(8)	(9)	(10)
Source	Position (1950.0)			Half-widths			Fig.	Henize	Base-
No.	R.A.	Dec.	$T_b(\text{max})$	R.A.	Dec.	$S_6$	No.	No.	level
	h m s	° ' "	(K)	' "	' "	(f.u.)			(K)
MC 1	04 24 36	-72 51.7	0.33	3.6	4.8	$0.53 \pm 0.15$	1		
MC 2	04 28 35	-67 55.2	0.20	<0.7	3.0	$0.24 \pm 0.06$	1		
MC 3	04 36 04	-74 56.8	0.21	<0.7	<0.7	$0.22 \pm 0.06$	1		
MC 4	04 36 20	-75 06.75	0.21	5.7	2.7	$0.37 \pm 0.06$	1		
MC 5	04 36 50	-65 03.6	0.32	<0.7	2.3	$0.38 \pm 0.06$	1		
MC 6	04 41 05	-69 57.3	0.23	4.1	2.8	$0.36 \pm 0.06$	1		
MC 7	04 43 14	-66 57.0	0.24	3.0	5.7	$0.44 \pm 0.07$	1		
MC 8	04 48 04	-69 20.5	0.10	<0.7	<0.7	$0.11 \pm 0.06$	3		
MC 9	04 49 10	-74 22.0	0.32	6.7	1.4	$0.55 \pm 0.06$	4		
MC 10	04 50 07	-69 16.5	0.19	<0.7	<0.7	$0.20 \pm 0.06$	3	77	
MC 11	04 50 49	-70 54.0	0.22	6.1	10.1	$0.41 \pm 0.15$	4		
MC 12	04 51 58	-66 59.8	0.24	<0.7	<0.7	$0.26 \pm 0.04$	2	4A	
MC 13	04 52 10	-69 27.0	0.41	4.9	5.1	$1.00 \pm 0.05$	3	79A	
MC 14	04 53 31	-67 17.1	0.23	3.3	5.9	$(0.51)$	2		
MC 15	04 53 32	-67 12.7	0.20	—	—		2		
MC 16	04 54 35	-69 15.8	0.41	4.8	3.0	$0.88 \pm 0.08$	3	83B	
MC 17	04 54 42	-64 54.3	0.32	3.5	4.6	$0.57 \pm 0.08$	4		
MC 18	04 56 44	-66 28.4	0.96	5.7	3.5	$3.37 \pm 0.30$	2	11	
MC 19	04 57 33	-68 29.5	0.31	2.1	5.9	$1.36 \pm 0.08$	3	91	
MC 20	05 04 45	-66 43.0	0.10	<0.7	<0.7	$0.11 \pm 0.06$	4		
MC 21	05 05 10	-66 57.5	0.12	<0.7	<0.7	$0.13 \pm 0.06$	4	20	
MC 22	05 09 06	-68 47.2	0.32	2.1	4.5	$0.53 \pm 0.06$	5	103A,B	
MC 23	05 10 04	-68 56.4	0.62	3.2	1.3	$0.90 \pm 0.06$	5	105A	
MC 24	05 13 37	-69 25.5	0.39	2.8	1.8	$0.62 \pm 0.06$	5	113C	
MC 25	05 14 33	-67 38.7	0.17	<0.7	5.7	$0.20 \pm 0.06$	4		
MC 26	05 15 32	-67 24.5	0.40	3.6	<0.7	$0.62 \pm 0.06$	4	33?	
MC 27	05 16 04	-72 39.6	0.22	1.8	3.8	$0.29 \pm 0.06$	4		
MC 28	05 17 07	-69 26.0	0.11	<0.7	<0.7	$0.12 \pm 0.06$	5		
MC 29	05 17 38	-72 39.8	0.34	<0.7	2.1	$0.40 \pm 0.06$	4		
MC 30	05 19 07	-69 16.4	0.33	4.7	8.1	$1.01 \pm 0.20$	5	119	
MC 31	05 19 37	-69 41.8	0.41	3.5	2.1	$0.70 \pm 0.06$	5	120A	
MC 32	05 22 05	-67 59.4	0.55	3.8	5.0	$1.21 \pm 0.10$	6	44	
MC 33	05 23 11	-68 04.9	0.31	3.8	5.0	$0.62 \pm 0.08$	6	44D	
MC 34	05 23 25	-65 49.8	0.18	<0.7	<0.7	$0.19 \pm 0.06$	7		
MC 35	05 23 28	-66 12.0	0.10	<0.7	<0.7	$0.11 \pm 0.66$	7		
MC 36	05 23 33	-66 23.8	0.10	—	—	$(0.10)$	7	46	
MC 37	05 24 15	-70 53.3	0.22	3.9	4.6	$0.38 \pm 0.08$	8		
MC 38	05 24 36	-69 54.5	0.18	<0.7	<0.7	$0.19 \pm 0.06$	5		
MC 39	05 25 26	-69 40.8	1.40	2.1	<0.7	$1.67 \pm 0.06$ $2.20 \pm 0.10^*$	5	132D	
MC 40	05 25 30	-66 20.9	0.33	3.0	4.1	$0.50 \pm 0.10$			
MC 41	05 25 53	-66 17.7	0.30	5.0	4.6	$0.66 \pm 0.10$	7	48B	
MC 42	05 25 58	-66 01.1	0.41	<0.7	3.9	$0.49 \pm 0.10$	7	48C	
MC 43	05 25 58	-66 06.8	0.91	<0.7	2.7	$1.03 \pm 0.10$	7	49	
MC 44	05 26 02	-65 51.8	0.17	—	—	$(0.10)$	7		
MC 45	05 26 08	-69 53.6	0.21	6.1	8.0	$0.76 \pm 0.10$	5	134	
MC 46	05 26 33	-67 30.8	0.26	7.2	3.9	$0.70 \pm 0.06$	6	51D	
MC 47	05 27 08	-68 50.6	0.33	3.0	4.7	$0.64 \pm 0.06$	5	144A	

\* Includes background contribution.

TABLE 1 (*Continued*)

(1)	(2)	(3)	(4)	(5)	(6)	(7)	(8)	(9)	(10)
Source	Position (1950.0)			Half-widths			Fig.	Henize	Base-
No.	R.A.	Dec.	$T_b(\text{max})$	R.A.	Dec.	$S_6$	No.	No.	level
	h m s	° ' "	(K)	' "	' "	(f.u.)			(K)
MC 48	05 27 29	-65 52.0	0.17	—	—	$0.22 \pm 0.06$	7		
MC 49	05 27 56	-65 06.5	0.19	3.8	2.1	$0.27 \pm 0.06$	9		
MC 50	05 27 56	-67 28.3	0.20	3.5	4.1	$0.36 \pm 0.06$	6	51A	
MC 51	05 27 57	-66 11.9	0.11	—	—	(0.13)	7		
MC 52	05 27 58	-66 30.1	0.10	—	—	(0.12)	7		
MC 53	05 30 24	-72 47.1	0.46	1.3	2.1	$0.54 \pm 0.06$	9		
MC 54	05 32 04	-71 05.8	0.44	6.6	4.9	$1.55 \pm 0.06$	8	206A	
MC 55	05 32 11	-68 42.5	0.18	—	—	$0.27 \pm 0.06$	6	148I	
MC 56	05 32 12	-68 32.8	0.15	—	—	$0.14 \pm 0.06$	6	148C	
MC 57	05 32 28	-67 42.6	0.31	6.8	4.6	$0.81 \pm 0.10$	6	57	
MC 58	05 32 30	-66 28.8	0.22	4.2	5.3	$0.48 \pm 0.06$	7	55	
MC 59	05 34 05	-65 55.0	0.22	<0.7	0.9	$0.20 \pm 0.07$	7		
MC 60	05 35 07	-65 53.4	0.29	<0.7	<0.7	$0.31 \pm 0.06$	7		
MC 61	05 35 10	-69 46.2	0.21	4.1	4.4	$0.39 \pm 0.06$	11	154	
MC 62	05 35 16	-66 17.8	0.18	<0.7	1.3	$0.16 \pm 0.06$	7	62A	
MC 63	05 35 28	-66 03.1	0.67	3.3	1.8	$0.90 \pm 0.10$ $1.15 \pm 0.06^*$	7	63	
MC 64	05 35 31	-67 36.0	1.10	1.8	2.1	$1.65 \pm 0.06$	6	59A	
MC 65	05 35 42	-69 30.8	0.24	—	—	(0.17)	11		0.1
MC 66	05 35 58	-66 25.7	0.18	3.8	4.5	$0.37 \pm 0.06$	7		
MC 67	05 36 00	-69 48.8	0.22	1.8	2.3	$0.31 \pm 0.10$	11		
MC 68	05 36 07	-68 58.0	0.28	—	—	(0.12)	11		0.1
MC 69	05 36 08	-69 14.2	0.84	5.4	8.0	$2.09 \pm 0.10$	11		0.2
MC 70	05 36 08	-69 32.7	0.23	—	—	(0.15)	11		0.1
MC 71	05 36 18	-69 40.3	0.45	<0.7	3.0	$0.55 \pm 0.06$	11	154A	0.1
MC 72	05 36 27	-69 30.75	0.22	—	—	(0.14)	11		0.1
MC 73	05 38 38	-69 23.1	0.42	—	—	$0.20 \pm 0.08$	11		0.2
MC 74	05 39 04	-69 06.5	12.6	3.0	3.0	25.14	11	157A	0.2
MC 75	05 39 37	-69 30.9	1.06	2.1	<0.7	$1.11 \pm 0.06$	11	158C	0.2
MC 76	05 40 09	-69 39.7	1.38	3.4	3.8	$1.80 \pm 0.10$	11	160A	0.2
MC 77	05 40 24	-69 46.0	1.80	2.1	<0.7	$1.93 \pm 0.10$	11	159	0.2
MC 78	05 40 40	-69 21.5	0.62	<0.7	0.9	$0.51 \pm 0.10$	11	158A	0.2
MC 79	05 42 32	-69 07.9	0.37	—	—	(0.15)	11		0.1
MC 80	05 42 34	-71 20.7	0.20	4.7	3.2	$0.37 \pm 0.06$	8	214C	
MC 81	05 42 49	-73 42.5	0.10	—	—	(0.12)	9		
MC 82	05 43 02	-69 05.3	0.38	—	—	(0.18)	6,11	164	0.1
MC 83	05 43 04	-73 32.5	0.67	<0.7	<0.7	$0.71 \pm 0.06$	9		
MC 84	05 43 39	-69 45.75	0.28	3.8	4.1	$0.50 \pm 0.06$	11	163	
MC 85	05 43 39	-68 57.9	0.20	1.8	4.3	$0.30 \pm 0.06$	6,11	165	
MC 86	05 44 04	-69 18.1	0.20	—	—	$0.12 \pm 0.06$	11		0.1
MC 87	05 45 55	-64 54.7	0.25	<0.7	<0.7	$0.30 \pm 0.06$	9		
MC 88	05 46 23	-64 35.3	0.12	—	—	(0.14)	9		
MC 89	05 47 30	-69 43.0	0.90	6.7	4.2	$1.00 \pm 0.10$	9		
MC 90	05 48 23	-70 04.0	0.24	<0.7	3.3	$0.26 \pm 0.06$	9	180C	
MC 91	05 49 27	-70 05.0	0.35	2.7	4.5	$0.61 \pm 0.08$	9	180A	
MC 92	05 51 05	-68 28.4	0.25	5.0	15.6	$1.55 \pm 0.10$	6		
MC 93	06 01 57	-70 35.0	0.25	2.1	1.6	$0.28 \pm 0.06$	10		
MC 94	06 02 24	-64 42.5	0.26	1.3	1.8	$0.30 \pm 0.06$	10		
MC 95	06 08 44	-65 50.5	0.40	2.8	2.7	$0.62 \pm 0.08$	10		

\* Includes background contribution.



The 6 cm integrated flux density  $S_6$  and its estimated standard error are given in column 7. Equation (1) was used for the calculation of the flux densities of point sources. However, the majority of sources were extended, and their flux densities were obtained by integrating the full-beam brightness temperature contours according to the relation

$$S = (2k/\lambda^2) \int T_b \, d\Omega = 0.65 \times 10^{-27} \int T_b \, d\Omega, \quad (2)$$

where  $\Omega$  is expressed in square minutes of arc and  $S$  is in  $\text{W m}^{-2} \text{Hz}^{-1}$ . Additional estimates of flux density were made by fitting Gaussian distributions to the contours of the sources by means of

$$S = 1.133 \Delta w_1 \Delta w_2 (2k/\lambda^2) T_b(\text{max}) = 0.74 \times 10^{-27} T_b(\text{max}) \Delta w_1 \Delta w_2, \quad (3)$$

where  $\Delta w_1$  and  $\Delta w_2$  are the apparent half-widths in minutes of arc.

The number of the figure in which the source is located is given in column 8. Catalogue numbers of LMC nebulae listed by Henize (1956) are shown in column 9 for those sources whose positions were less than  $3'$  arc from the nebulae. If the source was considered to be superimposed on background radiation the brightness temperature of the latter has been indicated as a baselevel in column 10.

#### V. ACKNOWLEDGMENTS

The authors were assisted in the early reductions by Mrs. Betty Siegman and Mrs. Peggy Lockhart, and the diagrams were traced by Mrs. Beth Nanlohy. They are particularly grateful to Miss Lynette Newton, who has ably performed all the work on the measurements and calculations shown in Table 1.

#### VI. REFERENCES

- BROTEN, N. W. (1965).—*Proc. Symp. on Magellanic Clouds*, Mt. Stromlo Obs., Canberra, pp. 72–5.  
 BROTEN, N. W. (1972).—*Aust. J. Phys.* **25**, 599–612.  
 CLARKE, J. N. (1971).—*Proc. astr. Soc. Aust.* **2**, 44–5.  
 COOPER, B. F. C. (1970).—*Proc. Instn Radio electron. Engrs Aust.* **31**, 41–8.  
 HENIZE, K. G. (1956).—*Astrophys. J. Suppl. Ser.* **2**, 315–44.  
 LE MARNE, A. E. (1968).—*Mon. Not. R. astr. Soc.* **139**, 461–9.  
 MCGEE, R. X., BROOKS, J. W., and BATCHELOR, R. A. (1972).—*Aust. J. Phys.* **25**, 613–17.  
 MCGEE, R. X., and NEWTON, LYNETTE M. (1972).—*Aust. J. Phys.* **25**, 619–35.  
 MATHEWSON, D. S., and HEALEY, J. R. (1964).—*Proc. I.A.U.—U.R.S.I. Symp. No. 20 on Galaxy and Magellanic Clouds*. (Eds. F. J. Kerr and A. W. Rodgers.) pp. 245–55.  
 MILLS, B. Y., and ALLER, L. H. (1971).—*Aust. J. Phys.* **24**, 609–15.  
 MILLS, B. Y., and LITTLE, A. G. (1953).—*Aust. J. Phys.* **6**, 272–8.  
 REIFENSTEIN, E. C. (1968).—Ph.D. Thesis, Massachusetts Institute of Technology.  
 THOMAS, B. MACA. (1970).—*Electron. Lett.* **6**, 461–2.

